POWER DISTRIBUTION SYSTEM OBSERVABILITY WITH SMART METER DATA

*Siddharth Bhela, Vassilis Kekatos**

Dept. of ECE, Virginia Tech,
Blacksburg, VA 24061, USA

Sriharsha Veeramachaneni

WindLogics Inc., 1021 Bandana Blvd E #111,
St Paul, MN 55108, USA

ABSTRACT

Power distribution system operators require knowledge of power injections for accomplishing various grid dispatch tasks. Monitoring, collecting, and processing smart meter data across all grid nodes however may not be affordable given the communication and storage resources. In this context, the problem of inferring injections at all nodes by polling smart meter data from a subset of them is considered here. For non-synchronized grid data, including (re)active injections and nodal voltage magnitudes, intuitive topological and numerical observability criteria are provided. For the case of synchrophasor data where nodal voltage angles are additionally known, the improvements in identifiability are also characterized. The analysis relies on the linearized power flow model and extends the traditional concept of observability in power transmission systems to radial distribution grids. The derived criteria are numerically validated on the IEEE 123-bus benchmark feeder.

***Index Terms*—** Smart meters, structural observability, linear distribution power flow, synchrophasor data.

1. INTRODUCTION

With the advent of distributed renewable generation, electric vehicles, and demand-response programs, network operators are in dire need of monitoring tools to track the power injections across all grid nodes to perform voltage regulation, power loss minimization, or optimal dispatch. Nonetheless, polling smart meter data on a network-wide basis is challenging due to limited bandwidth and computational resources.

The sheer size of residential distribution grids had made it cost-prohibitive to achieve observability. Meter placement schemes to improve distribution system state estimation have been reported in [1], [2], [3]. A heuristic rule aiming at reducing the variance of voltage magnitude and angle estimates at non-metered nodes is suggested in [2] and [3], respectively. Pseudo-measurements have also been used in restoring observability in distribution grids [4], and improving state estimation in medium-voltage networks [5]. The trade-off between state estimation accuracy and investment cost using synchrophasor and smart meter data is explored in [6].

*The work of S. Bhela has been supported by Windlogics Inc.

For a given measurement set, the identifiability of power transmission systems has been analyzed under the decoupled power flow model [7], [8]. Nonetheless, due to the higher resistance-to-reactance ratios, the latter model cannot be applied to distribution systems. The work in [9] investigates necessary and sufficient conditions for observability of a related power flow problem coupling two system states under the full AC model. This coupled problem exploits the variability at metered buses and the stationarity of conventional loads, to solve the non-linear power flow equations jointly over successive time instants. Different from the aforementioned setup, we are interested in system identifiability for a single time instant, under the linearized power flow model (LDF) introduced in [10], [11], [12].

Notation: Column vectors (matrices) are denoted using lower- (upper-) case boldface letters; and sets by calligraphic symbols; while $|\mathcal{X}|$ is the cardinality of set $\mathcal{X}$. The operator $(\cdot)^\top$ stands for transposition; $\mathrm{dg}(\mathbf{x})$ defines a diagonal matrix having $\mathbf{x}$ on its main diagonal; and $\mathrm{rk}(\cdot)$ is the matrix rank. The notation $\mathbf{x}_{\mathcal{A}}$ means the subvector of $\mathbf{x}$ indexed by the set $\mathcal{A}$, while $\mathbf{X}_{\mathcal{A},\mathcal{B}}$ is the matrix obtained by sampling the rows and columns of $\mathbf{X}$ indexed by subsets $\mathcal{A}$ and $\mathcal{B}$.

2. GRID MODELING

A distribution grid having $N+1$ buses can be represented by the graph $\mathcal{G}=(\mathcal{N}^+,\mathcal{L})$ with nodes $\mathcal{N}^+:=\{0,\ldots,N\}$ corresponding to grid buses, and edges $\mathcal{L}$ to distribution lines. For every bus $n\in\mathcal{N}^+$, let $\bar{u}_n=\bar{v}_n e^{j\theta_n}$ and i_n be the voltage and current phasors, and p_n+jq_n be the complex power injected from bus n to the grid. The substation bus is indexed by $n=0$ with $\theta_0=0$, while the remaining buses comprise set $\mathcal{N}$. The impedance for line $\ell\in\mathcal{L}$ is $r_\ell+jx_\ell$. The grid topology is captured by the branch-bus incidence matrix $\tilde{\mathbf{A}}\in\{0,\pm 1\}^{L\times(N+1)}$ that can be partitioned into its first column $\mathbf{a}_0$ and the *reduced incidence matrix* $\mathbf{A}$ as $\tilde{\mathbf{A}}=[\mathbf{a}_0\ \mathbf{A}]$.

To allow for a compact representation, collect quantities at all buses modulo the substation bus in the N-dimensional vectors $\boldsymbol{\theta}$, $\mathbf{i}$, and $\mathbf{p}+j\mathbf{q}$. Introduce also the real-valued vector $\mathbf{v}$ with entries $v_n:=\bar{v}_n-\bar{v}_0$ for $n\in\mathcal{N}$, and the complex-valued vector $\mathbf{u}$ with entries $u_n:=\bar{u}_n-\bar{v}_0$ again for $n\in\mathcal{N}$. Upon ignoring shunt elements, it can be readily shown that $\mathbf{i}=\mathbf{Y}\mathbf{u}$, where $\mathbf{Y}:=\mathbf{G}-j\mathbf{B}$ involves the reduced

conductance and susceptance matrices defined as

$$\mathbf{G} := \mathbf{A}^\top \operatorname{dg}\left(\left\{\frac{r_\ell}{r_\ell^2+x_\ell^2}\right\}_{\ell\in\mathcal{L}}\right)\mathbf{A} \tag{1a}$$

$$\mathbf{B} := \mathbf{A}^\top \operatorname{dg}\left(\left\{\frac{x_\ell}{r_\ell^2+x_\ell^2}\right\}_{\ell\in\mathcal{L}}\right)\mathbf{A}. \tag{1b}$$

Based on the first-order Taylor series expansion of the power flow equations, voltages can be approximated as [11], [12]:

$$\mathbf{v} \simeq \mathbf{R}\mathbf{p} + \mathbf{X}\mathbf{q} \tag{2a}$$

$$\boldsymbol{\theta} \simeq \mathbf{X}\mathbf{p} - \mathbf{R}\mathbf{q} \tag{2b}$$

where $\mathbf{R} := (\mathbf{G}+\mathbf{B}\mathbf{G}^{-1}\mathbf{B})^{-1}$ and $\mathbf{X} := (\mathbf{B}+\mathbf{G}\mathbf{B}^{-1}\mathbf{G})^{-1}$. For radial grids where $\mathbf{A}$ is square and invertible [13], the involved matrices simplify as $\mathbf{R} = (\mathbf{A}^\top \operatorname{dg}^{-1}(\{r_\ell\})\mathbf{A})^{-1}$ and $\mathbf{X} = (\mathbf{A}^\top \operatorname{dg}^{-1}(\{x_\ell\})\mathbf{A})^{-1}$. The (m,n)-th entry of $\mathbf{R}$, i.e., $\mathbf{R}_{mn}$, equals the sum of resistances for all common lines on the paths from buses n and m to the root bus. The same holds for $\mathbf{X}_{mn}$ if reactances are used in lieu of resistances [14]. The approximation in (2a) is known as the linear distribution flow (LDF) model [10], and numerical tests report approximation errors in voltage magnitudes less than 0.001 pu [15, 16].

2.1. Problem Statement

Conventionally, the voltage $\bar{v}_0$ at the substation bus is fixed and the remaining buses are modeled as PQ buses for which $\{(p_n, q_n)\}_{n\in\mathcal{N}}$ are specified [10]. This approach though does not apply when it comes to distributed resources and demand-response programs. In modern grids, it is more likely that all three quantities (p_n, q_n, v_n) are accessible in a subset $\mathcal{M} \subset \mathcal{N}$ of nodes whose smart meters are polled; whereas, for the remaining nodes comprising set $\bar{\mathcal{M}} := \mathcal{N} \setminus \mathcal{M}$, no information is available. Even if all buses are equipped with smart meters, not all meters can be polled due to bandwidth constraints. Our task is to discern whether for a given $\mathcal{M}$ it is possible to recover injections in $\bar{\mathcal{M}}$. Upon column and row permutations, the model in (2a) can be partitioned as:

$$\begin{bmatrix}\mathbf{v}_{\mathcal{M}}\\ \mathbf{v}_{\bar{\mathcal{M}}}\end{bmatrix} = \begin{bmatrix}\mathbf{R}_{\mathcal{M},\mathcal{M}} & \mathbf{R}_{\mathcal{M},\bar{\mathcal{M}}}\\ \mathbf{R}_{\bar{\mathcal{M}},\mathcal{M}} & \mathbf{R}_{\bar{\mathcal{M}},\bar{\mathcal{M}}}\end{bmatrix}\begin{bmatrix}\mathbf{p}_{\mathcal{M}}\\ \mathbf{p}_{\bar{\mathcal{M}}}\end{bmatrix} + \begin{bmatrix}\mathbf{X}_{\mathcal{M},\mathcal{M}} & \mathbf{X}_{\mathcal{M},\bar{\mathcal{M}}}\\ \mathbf{X}_{\bar{\mathcal{M}},\mathcal{M}} & \mathbf{X}_{\bar{\mathcal{M}},\bar{\mathcal{M}}}\end{bmatrix}\begin{bmatrix}\mathbf{q}_{\mathcal{M}}\\ \mathbf{q}_{\bar{\mathcal{M}}}\end{bmatrix}. \tag{3}$$

Apparently, given smart meter data $(\mathbf{v}_{\mathcal{M}}, \mathbf{p}_{\mathcal{M}}, \mathbf{q}_{\mathcal{M}})$, the unknown injections $(\mathbf{p}_{\bar{\mathcal{M}}}, \mathbf{q}_{\bar{\mathcal{M}}})$ can be uniquely recovered from the upper set of equations in (3) using the linear model:

$$\mathbf{v}_{\mathcal{M}} - \mathbf{R}_{\mathcal{M},\mathcal{M}}\mathbf{p}_{\mathcal{M}} - \mathbf{X}_{\mathcal{M},\mathcal{M}}\mathbf{q}_{\mathcal{M}} = \mathbf{H}_{\mathcal{M}}\begin{bmatrix}\mathbf{p}_{\bar{\mathcal{M}}}\\ \mathbf{q}_{\bar{\mathcal{M}}}\end{bmatrix} \tag{4}$$

if the involved matrix $\mathbf{H}_{\mathcal{M}} := [\mathbf{R}_{\mathcal{M},\bar{\mathcal{M}}}\ \mathbf{X}_{\mathcal{M},\bar{\mathcal{M}}}]$ is full column-rank. The rank of $\mathbf{H}_{\mathcal{M}}$ is studied next.

3. OBSERVABILITY ANALYSIS

Determining whether a distribution grid is observable given a set of smart meters $\mathcal{M}$ can be performed using topological or numerical methods. Some known results linking linear algebra to graph theory precede our observability analysis.

3.1. Preliminaries

A graph $\mathcal{G} = (\mathcal{V}, \mathcal{E})$ is *bipartite* if its vertex set $\mathcal{V}$ can be partitioned into two mutually exclusive and collectively exhaustive subsets $\mathcal{V}_1$ and $\mathcal{V}_2$ such that every edge $e \in \mathcal{E}$ connects a node in $\mathcal{V}_1$ with a node in $\mathcal{V}_2$. Moreover, a *matching* $\mathcal{Z} \subseteq \mathcal{E}$ is a subset of edges in $\mathcal{G}$ so that each node in $\mathcal{V}$ appears in at most one edge in $\mathcal{Z}$. A matching is *perfect* if each node in $\mathcal{V}$ has exactly one edge incident to it.

The analysis is based on the *generic rank* of a matrix, defined as the maximum possible rank attained if the non-zero entries of this matrix are allowed to take arbitrary values in $\mathbb{R}$ [17], [18]. An $N \times N$ matrix is termed generically invertible if its generic rank is N. Let us associate matrix $\mathbf{E} \in \mathbb{R}^{N\times N}$ with a bipartite graph $\mathcal{G}$ having $2N$ nodes. Each column of $\mathbf{E}$ is mapped to a column node, and each row of $\mathbf{E}$ to a row node. An edge runs from the n-th column node to the m-th row node only if $\mathbf{E}_{m,n} \neq 0$. Lemma 1 builds on $\mathcal{G}$.

Lemma 1 ([17])**.** *Matrix* $\mathbf{E}$ *is generically invertible if and only if the bipartite graph* $\mathcal{G}$ *has a perfect matching.*

The result extends to block-partitioned matrices [18]. Partition matrix $\mathbf{E}$ as

$$\mathbf{E} = \begin{bmatrix}\mathbf{A} & \mathbf{B}\\ \mathbf{C} & \mathbf{D}\end{bmatrix} \tag{5}$$

where $\mathbf{A} \in \mathbb{R}^{M\times M}$, $\mathbf{B} \in \mathbb{R}^{M\times K}$, $\mathbf{C} \in \mathbb{R}^{T\times M}$, and $\mathbf{D} \in \mathbb{R}^{T\times K}$ with $T \geq K$. To characterize the generic rank of $\mathbf{E}$, the next result can be invoked [19, p. 25]:

Lemma 2 (Rank additivity)**.** *If* $\mathbf{A}$ *in* (5) *is invertible, then it holds that* $\operatorname{rk}(\mathbf{E}) = \operatorname{rk}(\mathbf{A}) + \operatorname{rk}(\mathbf{D} - \mathbf{C}\mathbf{A}^{-1}\mathbf{B})$.

The next holds for the rank of a matrix product [19].

Lemma 3 (Sylvester's inequality)**.** *If* $\mathbf{F} \in \mathbb{R}^{M\times K}$ *and* $\mathbf{T} \in \mathbb{R}^{K\times P}$*, it holds that* $\operatorname{rk}(\mathbf{F}) + \operatorname{rk}(\mathbf{T}) - K \leq \operatorname{rk}(\mathbf{F}\mathbf{T}) \leq \min\{\operatorname{rk}(\mathbf{F}), \operatorname{rk}(\mathbf{T})\}$.

It follows from Lemma 3 that if $P \leq K \leq M$ and $(\mathbf{F}, \mathbf{T})$ are both full rank, then $\operatorname{rk}(\mathbf{F}\mathbf{T}) = P$.

3.2. Topological and Numerical Observability

A necessary condition for the linear model in (4) to be identifiable is that matrix $\mathbf{H}_{\mathcal{M}}$ is tall implying that $|\mathcal{M}| \geq 2|\bar{\mathcal{M}}|$. This section considers the case where $|\mathcal{M}| = 2|\bar{\mathcal{M}}|$; if $|\mathcal{M}| > 2|\bar{\mathcal{M}}|$, our analysis relies on the existence of an appropriate subset $\mathcal{M}_s \subseteq \mathcal{M}$ such that $|\mathcal{M}_s| = 2|\bar{\mathcal{M}}|$. We first study $\operatorname{rk}(\mathbf{R}_{\mathcal{M},\bar{\mathcal{M}}})$ – with the same analysis carrying over to $\mathbf{X}_{\mathcal{M},\bar{\mathcal{M}}}$ – and subsequently $\operatorname{rk}(\mathbf{H}_{\mathcal{M}})$.

Proposition 1. *Consider the graph $\mathcal{T}'$ derived from the tree $\mathcal{T} = (\mathcal{N}^+, \mathcal{L})$ by removing the substation bus and its incident edges. Without loss of generality, graph $\mathcal{T}'$ is assumed to be a tree. Matrix $\mathbf{R}_{\mathcal{M},\bar{\mathcal{M}}}$ is generically full column-rank if and only if there exists a perfect matching from $\bar{\mathcal{M}}$ to $\mathcal{M}$ on $\mathcal{T}'$.*

Proof. Partition matrix $\mathbf{L} := \mathbf{R}^{-1}$ conformably to (3) as

$$\mathbf{L} = \begin{bmatrix} \mathbf{L}_{\mathcal{M},\mathcal{M}} & \mathbf{L}_{\mathcal{M},\bar{\mathcal{M}}} \\ \mathbf{L}_{\bar{\mathcal{M}},\mathcal{M}} & \mathbf{L}_{\bar{\mathcal{M}},\bar{\mathcal{M}}} \end{bmatrix}. \tag{6}$$

Matrices $\mathbf{L}$ and $\mathbf{L}_{\mathcal{M},\mathcal{M}}$ are principal minors of the grid graph Laplacian, and are hence invertible [13]. Since $\mathrm{rk}(\mathbf{L}) = N$ and $\mathrm{rk}(\mathbf{L}_{\mathcal{M},\mathcal{M}}) = M$, Lemma 2 implies that the Schur complement of $\mathbf{L}$ with respect to $\mathbf{L}_{\mathcal{M},\mathcal{M}}$ defined as

$$\bar{\mathbf{L}}_{\bar{\mathcal{M}},\bar{\mathcal{M}}} := \mathbf{L}_{\bar{\mathcal{M}},\bar{\mathcal{M}}} - \mathbf{L}_{\bar{\mathcal{M}},\mathcal{M}} \mathbf{L}^{-1}_{\mathcal{M},\mathcal{M}} \mathbf{L}_{\mathcal{M},\bar{\mathcal{M}}} \tag{7}$$

is of full rank $N-M$. Since $\mathbf{L}_{\mathcal{M},\mathcal{M}}$ and $\bar{\mathbf{L}}_{\bar{\mathcal{M}},\bar{\mathcal{M}}}$ are invertible, the matrix inversion lemma for blocked matrices yields [19]

$$\mathbf{R}_{\mathcal{M},\bar{\mathcal{M}}} = -\mathbf{L}^{-1}_{\mathcal{M},\mathcal{M}} \mathbf{L}_{\mathcal{M},\bar{\mathcal{M}}} \bar{\mathbf{L}}^{-1}_{\bar{\mathcal{M}},\bar{\mathcal{M}}}.$$

Consequently, it stems from Lemma 3 that $\mathbf{R}_{\mathcal{M},\bar{\mathcal{M}}}$ is full-rank if and only if $\mathbf{L}_{\mathcal{M},\bar{\mathcal{M}}}$ is full-rank. Observe that $\mathbf{L}_{\mathcal{M},\bar{\mathcal{M}}}$ has non-zero entries only if the nodes in $\bar{\mathcal{M}}$ are adjacent to the nodes in $\mathcal{M}$. The generic rank of $\mathbf{L}_{\mathcal{M},\bar{\mathcal{M}}}$ can then be characterized by Lemma 1. In detail, matrix $\mathbf{L}_{\mathcal{M},\bar{\mathcal{M}}}$ and therefore matrix $\mathbf{R}_{\mathcal{M},\bar{\mathcal{M}}}$ are generically invertible if and only if the criterion in Prop. 1 is met. □

To verify our analysis consider two leaf nodes in $\bar{\mathcal{M}}$ with the same parent node in $\mathcal{T}'$. This scenario not only fails to satisfy Prop. 1 for topological observability, but breaks down numerically as well. To check numerical observability, recall that the entry $\mathbf{R}_{mn}$ equals the sum of resistances for all common ancestors of buses n and m up to the substation. Therefore, if any two nodes $n, k \in \bar{\mathcal{M}}$ have the same ancestors with respect to every node in $\mathcal{M}$, then the n-th and k-th columns of $\mathbf{R}_{\mathcal{M},\bar{\mathcal{M}}}$ are identical. Having characterized the rank of $\mathbf{R}_{\mathcal{M},\bar{\mathcal{M}}}$, the attention is next focused on $\mathbf{H}_{\mathcal{M}}$.

Proposition 2. *Matrix $\mathbf{H}_{\mathcal{M}}$ is generically invertible if every node in $\bar{\mathcal{M}}$ is connected to a unique node in $\mathcal{M}_1$ and a unique node in $\mathcal{M}_2$ with $\mathcal{M}_1 \cup \mathcal{M}_2 = \mathcal{M}$ and $\mathcal{M}_1 \cap \mathcal{M}_2 = \emptyset$ on graph $\mathcal{T}'$.*

Proof. Partition $\mathcal{M}$ into two subsets $\mathcal{M}_1$ and $\mathcal{M}_2$ of equal cardinality. Then, matrix $\mathbf{H}_{\mathcal{M}}$ can be expressed as

$$\mathbf{H}_{\mathcal{M}} = \begin{bmatrix} \mathbf{R}_{\mathcal{M}_1,\bar{\mathcal{M}}} & \mathbf{X}_{\mathcal{M}_1,\bar{\mathcal{M}}} \\ \mathbf{R}_{\mathcal{M}_2,\bar{\mathcal{M}}} & \mathbf{X}_{\mathcal{M}_2,\bar{\mathcal{M}}} \end{bmatrix}. \tag{8}$$

If the top-left and bottom-right blocks of $\mathbf{H}_{\mathcal{M}}$ in (8) are full-rank, then Lemma 1 asserts that $\mathbf{H}_{\mathcal{M}}$ is of full generic rank. To characterize the full-rank condition for the top-left block $\mathbf{R}_{\mathcal{M}_1,\bar{\mathcal{M}}}$, partition now matrix $\mathbf{L}$ as

$$\mathbf{L} = \begin{bmatrix} \mathbf{L}_{\mathcal{M}_1,\bar{\mathcal{M}}} & \mathbf{L}_{\mathcal{M}_1,\mathcal{M}} \\ \mathbf{L}_{\mathcal{M}_2\cup\bar{\mathcal{M}},\bar{\mathcal{M}}} & \mathbf{L}_{\mathcal{M}_2\cup\bar{\mathcal{M}},\mathcal{M}} \end{bmatrix}. \tag{9}$$

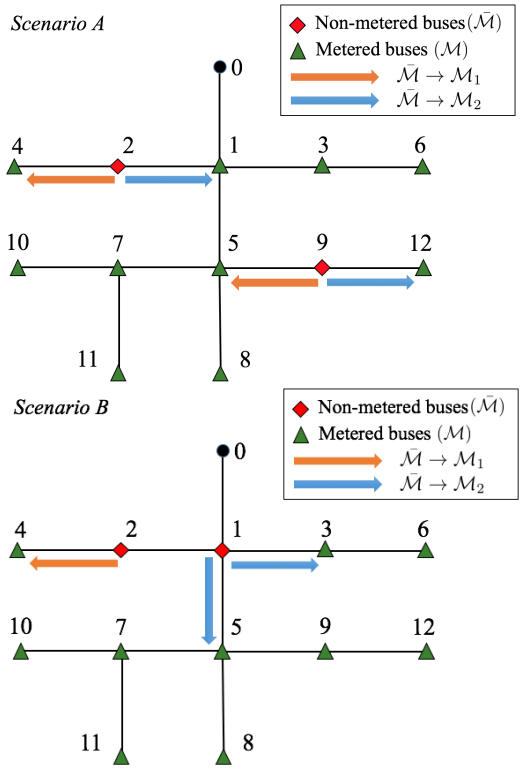

Fig. 1: Operating scenarios for the IEEE 13-bus grid [20]: Scenario A satisfies Prop. 1 and 2; Scenario B fails Prop. 2.

Unlike the partitioning in (6) where $\mathbf{L}_{\mathcal{M},\mathcal{M}}$ is invertible, block $\mathbf{L}_{\mathcal{M}_1,\bar{\mathcal{M}}}$ is generically invertible if and only if there exists a perfect matching between $\bar{\mathcal{M}}$ and $\mathcal{M}_1$. Similarly, block $\mathbf{L}_{\mathcal{M}_2\cup\bar{\mathcal{M}},\mathcal{M}} = \mathbf{L}_{\mathcal{M}_2\cup\bar{\mathcal{M}},\mathcal{M}_1\cup\mathcal{M}_2}$ is also invertible under the same criterion, as the set $\mathcal{M}_2$ can be mapped to itself. It then follows that $\mathbf{L}$ is invertible under Lemma 1. Because matrices $\mathbf{L}$ and $\mathbf{L}_{\mathcal{M}_2\cup\bar{\mathcal{M}},\mathcal{M}}$ are invertible under Prop. 2, Lemma 2 implies that the Schur complement of $\mathbf{L}$ with respect to the latter is invertible as well. Then using the matrix inversion lemma for blocked matrices [19], it follows that the ensuing matrix is generically of full rank:

$$\mathbf{R}_{\mathcal{M}_1,\bar{\mathcal{M}}} = (\mathbf{L}_{\mathcal{M}_1,\bar{\mathcal{M}}} - \mathbf{L}_{\mathcal{M}_1,\mathcal{M}} \mathbf{L}^{-1}_{\mathcal{M}_2\cup\bar{\mathcal{M}},\mathcal{M}} \mathbf{L}_{\mathcal{M}_2\cup\bar{\mathcal{M}},\bar{\mathcal{M}}})^{-1}.$$

To complete the proof, we now characterize the conditions for the invertibility of $\mathbf{X}_{\mathcal{M}_2,\bar{\mathcal{M}}}$ in (8). Partition $\mathbf{U} := \mathbf{X}^{-1}$ as

$$\mathbf{U} = \begin{bmatrix} \mathbf{U}_{\mathcal{M},\bar{\mathcal{M}}} & \mathbf{U}_{\mathcal{M},\mathcal{M}} \\ \mathbf{U}_{\bar{\mathcal{M}},\bar{\mathcal{M}}} & \mathbf{U}_{\bar{\mathcal{M}},\mathcal{M}} \end{bmatrix} = \begin{bmatrix} \mathbf{U}_{\mathcal{M}_2,\bar{\mathcal{M}}} & \mathbf{U}_{\mathcal{M}_2,\mathcal{M}} \\ \mathbf{U}_{\mathcal{M}_1\cup\bar{\mathcal{M}},\bar{\mathcal{M}}} & \mathbf{U}_{\mathcal{M}_1\cup\bar{\mathcal{M}},\mathcal{M}} \end{bmatrix}.$$

Utilizing the same arguments used to identify the full rank condition of $\mathbf{R}_{\mathcal{M}_1,\bar{\mathcal{M}}}$, matrix $\mathbf{X}_{\mathcal{M}_2,\bar{\mathcal{M}}} = (\mathbf{U}_{\mathcal{M}_2,\bar{\mathcal{M}}} - \mathbf{U}_{\mathcal{M}_2,\mathcal{M}} \mathbf{U}^{-1}_{\mathcal{M}_1\cup\bar{\mathcal{M}},\mathcal{M}} \mathbf{U}_{\mathcal{M}_1\cup\bar{\mathcal{M}},\bar{\mathcal{M}}})^{-1}$ is generically invertible if and only if there exists a perfect matching between $\bar{\mathcal{M}}$ and $\mathcal{M}_2$. Hence, matrices $\mathbf{R}_{\mathcal{M}_1,\bar{\mathcal{M}}}$ and $\mathbf{X}_{\mathcal{M}_2,\bar{\mathcal{M}}}$ are invertible under Prop. 2 and it follows that $\mathbf{H}_{\mathcal{M}}$ is generically full rank under Lemma 1. □

The established criteria in Props. 1–2 rely on finding mappings between $\bar{\mathcal{M}}$ and $\mathcal{M}$ on the graph derived by maintaining only the edges $\mathcal{L}$ running between $\bar{\mathcal{M}}$ and $\mathcal{M}$ on $\mathcal{T}'$. This bipartite matching problem an be solved as a maximum network flow problem using the Ford-Fulkerson algorithm [21]. The maxflow algorithm not only yields the size of the matching, but also identifies the edges used in the matching. This is helpful in identifying problematic nodes, i.e., nodes that do not meet the matching criterion.

Suppose $\bar{\mathcal{M}} = \{2, 9\}$, $\mathcal{M}_1 = \{4, 5\}$, and $\mathcal{M}_2 = \{1, 12\}$, shown as Scenario A in Fig. 1. Since the paths $(2-4, 9-5)$ connect every node in $\bar{\mathcal{M}}$ to a unique node in $\mathcal{M}_1$ and the paths $(2-1, 9-12)$, connect every node in $\bar{\mathcal{M}}$ to a unique node in $\mathcal{M}_2$, the linearized power flow problem is invertible. Consider now the case where $\bar{\mathcal{M}} = \{1, 2\}$ shown as Scenario B in Fig. 1. Although, Prop. 1 is met, there is no partitioning of $\mathcal{M}$ into two subsets such that Prop. 2 can be satisfied.

Even if Prop. 2 is met, matrix $\mathbf{H}_{\mathcal{M}}$ could be numerically rank-deficient. For example, if the line resistance-to-reactance ratios r_ℓ/x_ℓ are constant for the common ancestors of any node $n \in \bar{\mathcal{M}}$ with respect to every node in $\mathcal{M}$, then the n-th column of $\mathbf{R}_{\mathcal{M},\bar{\mathcal{M}}}$ will be a scalar multiple of the n-th column of $\mathbf{X}_{\mathcal{M},\bar{\mathcal{M}}}$. While distribution grids have many lines with similar ratios, it is unlikely that they are all constant. Also note that if any two nodes $n, k \in \bar{\mathcal{M}}$ have the same ancestors with respect to every node in $\mathcal{M}$, the n-th and k-th columns of $\mathbf{H}_{\mathcal{M}}$ are identical.

We now consider the observability analysis assuming PMU data on $\mathcal{M}$. While smart meters are only able to measure (p_n, q_n, v_n), PMUs can additionally collect the voltage angles θ_n. Interestingly, it will be shown that by adding voltage angle measurements, the sufficient condition for invertibility can be relaxed from Prop. 2 back to Prop. 1.

Consider the LDF model in (2) and the subsequent expansion and partitioning

$$\begin{bmatrix} \mathbf{v}_{\mathcal{M}} \\ \mathbf{v}_{\bar{\mathcal{M}}} \\ \boldsymbol{\theta}_{\mathcal{M}} \\ \boldsymbol{\theta}_{\bar{\mathcal{M}}} \end{bmatrix} = \begin{bmatrix} \mathbf{R}_{\mathcal{M},\mathcal{M}} & \mathbf{R}_{\mathcal{M},\bar{\mathcal{M}}} \\ \mathbf{R}_{\bar{\mathcal{M}},\mathcal{M}} & \mathbf{R}_{\bar{\mathcal{M}},\bar{\mathcal{M}}} \\ \mathbf{X}_{\mathcal{M},\mathcal{M}} & \mathbf{X}_{\mathcal{M},\bar{\mathcal{M}}} \\ \mathbf{X}_{\bar{\mathcal{M}},\mathcal{M}} & \mathbf{X}_{\bar{\mathcal{M}},\bar{\mathcal{M}}} \end{bmatrix} \begin{bmatrix} \mathbf{p}_{\mathcal{M}} \\ \mathbf{p}_{\bar{\mathcal{M}}} \end{bmatrix} + \begin{bmatrix} \mathbf{X}_{\mathcal{M},\mathcal{M}} & \mathbf{X}_{\mathcal{M},\bar{\mathcal{M}}} \\ \mathbf{X}_{\bar{\mathcal{M}},\mathcal{M}} & \mathbf{X}_{\bar{\mathcal{M}},\bar{\mathcal{M}}} \\ -\mathbf{R}_{\mathcal{M},\mathcal{M}} & -\mathbf{R}_{\mathcal{M},\bar{\mathcal{M}}} \\ -\mathbf{R}_{\bar{\mathcal{M}},\mathcal{M}} & -\mathbf{R}_{\bar{\mathcal{M}},\bar{\mathcal{M}}} \end{bmatrix} \begin{bmatrix} \mathbf{p}_{\mathcal{M}} \\ \mathbf{q}_{\bar{\mathcal{M}}} \end{bmatrix}. \tag{10}$$

Define $\boldsymbol{\alpha}_{\mathcal{M}} := \mathbf{v}_{\mathcal{M}} - \mathbf{R}_{\mathcal{M},\mathcal{M}}\mathbf{p}_{\mathcal{M}} - \mathbf{X}_{\mathcal{M},\mathcal{M}}\mathbf{q}_{\mathcal{M}}$ and $\boldsymbol{\gamma}_{\mathcal{M}} := \boldsymbol{\theta}_{\mathcal{M}} - \mathbf{X}_{\mathcal{M},\mathcal{M}}\mathbf{p}_{\mathcal{M}} + \mathbf{R}_{\mathcal{M},\mathcal{M}}\mathbf{q}_{\mathcal{M}}$. Given $(\mathbf{v}_{\mathcal{M}}, \boldsymbol{\theta}_{\mathcal{M}}, \mathbf{p}_{\mathcal{M}}, \mathbf{q}_{\mathcal{M}})$, the unknown injections $(\mathbf{p}_{\bar{\mathcal{M}}}, \mathbf{q}_{\bar{\mathcal{M}}})$ can be uniquely recovered from the first and third set of equations in (10)

$$\begin{bmatrix} \boldsymbol{\alpha}_{\mathcal{M}} \\ \boldsymbol{\gamma}_{\mathcal{M}} \end{bmatrix} = \begin{bmatrix} \tilde{\mathbf{H}}_{\mathcal{M}} \end{bmatrix} \begin{bmatrix} \mathbf{p}_{\bar{\mathcal{M}}} \\ \mathbf{q}_{\bar{\mathcal{M}}} \end{bmatrix} \tag{11}$$

if the involved matrix

$$\tilde{\mathbf{H}}_{\mathcal{M}} = \begin{bmatrix} \mathbf{R}_{\mathcal{M},\bar{\mathcal{M}}} & \mathbf{X}_{\mathcal{M},\bar{\mathcal{M}}} \\ \mathbf{X}_{\mathcal{M},\bar{\mathcal{M}}} & -\mathbf{R}_{\mathcal{M},\bar{\mathcal{M}}} \end{bmatrix} \tag{12}$$

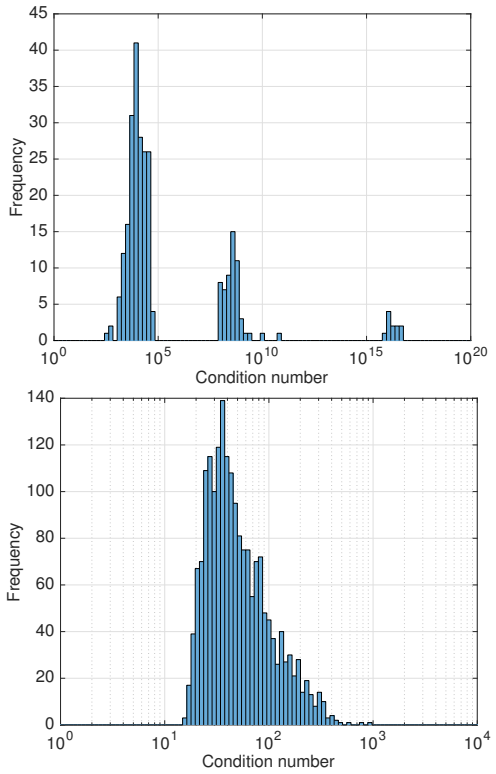

Fig. 2: Histograms of condition numbers.

is full column rank. A necessary condition is that $\tilde{\mathbf{H}}_{\mathcal{M}}$ is tall implying that $|\mathcal{M}| \geq |\bar{\mathcal{M}}|$. Since $\mathbf{R}_{\mathcal{M},\bar{\mathcal{M}}}$ is invertible under Prop. 1, matrix $\tilde{\mathbf{H}}_{\mathcal{M}}$ is full column rank under the same criterion. To see this, observe that $\mathbf{R}_{\mathcal{M},\bar{\mathcal{M}}}$ appears on the block diagonal of $\tilde{\mathbf{H}}_{\mathcal{M}}$, thus if $\mathbf{R}_{\mathcal{M},\bar{\mathcal{M}}}$ is invertible, then $\tilde{\mathbf{H}}_{\mathcal{M}}$ is full rank under Lemma 1. Observe that Scenario B in Fig. 1 will not fail the topological or numerical observability test if synchronized angle measurements are available.

4. NUMERICAL TESTS & CONCLUSIONS

The derived observability criteria were tested by checking the condition number of $\mathbf{H}_{\mathcal{M}}$ and $\tilde{\mathbf{H}}_{\mathcal{M}}$ constructed by randomly placing $|\bar{\mathcal{M}}| = 4$ buses on the IEEE 123-bus feeder [20]. The top part of Fig. 2 reports the condition numbers of $\mathbf{H}_{\mathcal{M}}$ when Prop. 2 was met; the higher condition numbers were attributed to the cases where the matrix is numerically rank-deficient. The bottom part of Fig. 2 reports the condition number of $\tilde{\mathbf{H}}_{\mathcal{M}}$. In conclusion, the topological criterion offers a sufficient condition for $\mathbf{H}_{\mathcal{M}}$ and $\tilde{\mathbf{H}}_{\mathcal{M}}$ to be full column-rank, while the numerical criterion provided some intuition behind the circumstances under which these matrices may be rank-deficient. The criteria also indicate that the ideal setup of allowing 1/3 of smart meters non-polled (1/2 for PMUs) is constrained by the grid topology. Finally, the graph matching algorithms reveal which nodes are unobservable and can be used for designing smart meter polling schemes.

5. REFERENCES

[1] M. E. Baran, J. Zhu, and A. W. Kelley, "Meter placement for real-time monitoring of distribution feeders," *IEEE Trans. Power Syst.*, vol. 11, no. 1, pp. 332–337, Feb. 1996.

[2] A. Shafiu, N. Jenkins, and G. Strbac, "Measurement location for state estimation of distribution networks with generation," in *IEE Proceedings - Gen., Trans. and Dist.*, vol. 152, no. 2, Mar. 2005, pp. 240–246.

[3] R. Singh, B. Pal, and R. Vinter, "Measurement placement in distribution system state estimation," in *Proc. IEEE Power & Energy Society General Meeting*, Calgary, AB, Jul. 2009.

[4] K. A. Clements, "The impact of pseudo-measurements on state estimator accuracy," in *Proc. IEEE Power & Energy Society General Meeting*, Detroit, MI, Jul. 2011.

[5] J. Wu, Y. He, and N. Jenkins, "A robust state estimator for medium voltage distribution networks," *IEEE Trans. Power Syst.*, vol. 28, no. 2, pp. 1008–1016, May 2013.

[6] J. Liu, J. Tang, F. Ponci, A. Monti, C. Muscas, and P. A. Pegoraro, "Trade-offs in PMU deployment for state estimation in active distribution grids," *IEEE Trans. Smart Grid*, vol. 3, no. 2, pp. 915–924, Jun. 2012.

[7] A. Monticelli, "Electric power system state estimation," *Proc. IEEE*, vol. 88, no. 2, pp. 262–282, Feb. 2000.

[8] Y. Guo, B. Zhang, W. Wu, Q. Guo, and H. Sun, "Solvability and solutions for bus-type extended load flow," *Intl. Journal of Electrical Power & Energy Systems*, vol. 51, pp. 89–97, 2013.

[9] S. Bhela, V. Kekatos, and S. Veeramachaneni, "Enhancing observability in distribution grids using smart meter data," *IEEE Trans. Smart Grid*, vol. PP, no. 99, pp. 1–1, 2017.

[10] M. Baran and F. Wu, "Network reconfiguration in distribution systems for loss reduction and load balancing," *IEEE Trans. Power Del.*, vol. 4, no. 2, pp. 1401–1407, Apr. 1989.

[11] D. Deka, S. Backhaus, and M. Chertkov, "Structure learning and statistical estimation in distribution networks — Part I," 2015, (submitted). [Online]. Available: http://arxiv.org/abs/1501.04131

[12] S. Bolognani and F. Dorfler, "Fast power system analysis via implicit linearization of the power flow manifold," Allerton, IL, Sep. 2015, pp. 402–409.

[13] C. Godsil and G. Royle, *Algebraic Graph Theory*. New York, NY: Springer, 2001.

[14] M. Farivar, L. Chen, and S. Low, "Equilibrium and dynamics of local voltage control in distribution systems," in *Proc. IEEE Conf. on Decision and Control*, Florence, Italy, Dec. 2013, pp. 4329–4334.

[15] L. Gan, N. Li, U. Topcu, and S. Low, "On the exactness of convex relaxation for optimal power flow in tree networks," in *Proc. IEEE Conf. on Decision and Control*, Maui, HI, Dec. 2012, pp. 465–471.

[16] V. Kekatos, L. Zhang, G. B. Giannakis, and R. Baldick, "Voltage regulation algorithms for multiphase power distribution grids," *IEEE Trans. Power Syst.*, vol. 31, no. 5, pp. 3913–3923, Sep. 2016.

[17] W. T. Tutte, "The factorization of linear graphs," *Journal of the London Mathematical Society*, vol. 22, no. 2, pp. 107–111, 1947.

[18] J.-M. Dion, C. Commault, and J. van der Woude, "Survey generic properties and control of linear structured systems: A survey," *Automatica*, vol. 39, no. 7, pp. 1125–1144, Jul. 2003.

[19] R. A. Horn and C. R. Johnson, *Topics in Matrix Analysis*. Cambridge University Press, 2013.

[20] W. H. Kersting, "Radial distribution test feeders," in *Proc. Power Engineering Society Winter Meeting*, vol. 2, 2001, pp. 908–912.

[21] L. R. Ford and D. R. Fulkerson, "Maximal flow through a network," *Canadian Journal of Mathematics*, vol. 8, pp. 399–404, 1956.